Food Chemistry: X 24 (2024) 102021

Contents lists available at ScienceDirect

Food Chemistry: X

journal homepage: www.sciencedirect.com/journal/food-chemistry-x

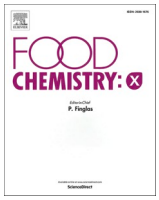

An integrative multi-omics approach reveals metabolic mechanism of flavonoids during anaerobic fermentation of de'ang pickled tea

Honglin Mao [a,1], Yang Xu [b,1], Fengmei Lu [c], Cunqiang Ma [d], Shaoxian Zhu [a], Guoyou Li [a], Siqi Huang [a], Yi Zhang [c], Yan Hou [e,*]

[a] College of Food Science and Technology, Yunnan Agricultural University, Kunming 650201, Yunnan, China
[b] International College, Yunnan Agricultural University, Kunming 650201, Yunnan, China
[c] Yunnan Defeng Tea Industry Co., Ltd, Mangshi 678400, Yunnan, China
[d] College of Horticulture, Nanjing Agricultural University, Nanjing 210095, Jiangsu, China
[e] College of Tea Science, Yunnan Agricultural University, Kunming 650201, Yunnan, China

ARTICLE INFO

Keywords:
Dark tea
Widely targeted metabolomics
LAB
Candida metapsilosis
Flavonols
Correlation analysis

ABSTRACT

Anaerobic fermentation (AF) is critical process for Yunnan De'ang pickled tea production. Therefore, widely targeted metabolomics and metagenomics were integrated to reveal the AF mechanism. Lactic acid bacteria (LAB) (e.g. *Lactiplantibacillus plantarum*, *Lactobacillus vaccinostercus* and *Lactobacillus paracollinoides*) and yeasts like *Candida metapsilosis* and *Cyberlindnera fabianii* dominated in the AF. Based on bacterial community succession and metabolites variation, the whole AF processes were divided into two phases, i.e., before and after four months. A total of 327 characteristic metabolites (VIP >1.0, $P < 0.05$, and FC > 1.50 or < 0.67) were selected from the AF. Besides amino acids increase, LAB and yeasts also promoted non-galloylated catechins, and several simple flavones/flavonols, flavanones/flavanonols and methoxy flavones/flavonols accumulations along with galloylated catechins, flavonol/flavone glycosides and anthocyanins decrease during the AF. This study would improve the understanding about AF mechanism of tea-leaves from the perspectives of flavonoids metabolism and microbial community succession.

1. Introduction

Dark teas (post-fermented teas) have been popular recently for multiple health benefits such as anti-obesity, anti-diabetic and anti-cancer activity (Lin et al., 2021), and can be basically divided into two main types: aerobic and anaerobic (Zhang et al., 2019). For example, despite both made from fresh tea-leaves of Yunnan Dayezhong variety (*Camellia sinensis* var. *assamica*), ripened Pu-erh tea (RPT) and Yunnan De'ang pickled tea (YDPT) show remarkable differences in chemical composition and sensory quality (Ma et al., 2023; Wen et al., 2023). The former is made through pile-fermentation for about 35 days under natural aerobic condition, while the latter produced by anaerobic fermentation (AF) for about nine months (Ma et al., 2023; Wen et al., 2023). At present, the multi-omics with the integration of metagenomics and metabolomics has been developed to explore the pile-fermentation or aerobic fermentation mechanism of dark teas including RPT (Zhao et al., 2019), Qingzhuan tea (Cheng et al., 2024) and Liupao tea (Pan et al., 2023). Our previous study (Hou et al., 2023) confirmed the increase of total phenolics and amino acids contents in YDPT processing, due to special fermentation process, i.e., the AF. However, the AF mechanism such as metabolites conversion rule, microbial community succession and their potential connections, has not been revealed yet.

Generally, *Aspergillus* as dominant fungi in the pile-fermentation, promotes the structural modification and oxidative polymerization of catechins (flavan-3-ols) for phenolics decrease, the glycosylation and hydrolyzation of flavonoids, the accumulation and *O*-methylation of phenolic acids, and the degradation and *N*-acetylation of amino acids through multifarious extracellular enzymes, including polyphenol oxidase, peroxidases, tannase, pectinases, cellulases, laccases, glycoside hydrolases, glycosyltransferases and transmethylase (Ma et al., 2021; Ma et al., 2024; Xu, Wei, Li, & Wei, 2022). Conversely, a completely different microbial community structure has been found in the AF. For instance, *Lactobacillus* (29.2–77.2 %) and *Acetobacter* (3.8–22.8 %) were dominated in bacteria, while *Candida* (72.5–89.0 %) and *Pichia*

* Corresponding author at: Yunnan Agricultural University, China.
E-mail address: zgynndhy@163.com (Y. Hou).
[1] The authors contributed equally to this work.

https://doi.org/10.1016/j.fochx.2024.102021
Received 13 September 2024; Received in revised form 13 November 2024; Accepted 17 November 2024
Available online 20 November 2024

(8.1–14.9 %) were dominant fungal genera during the AF of Miang (Unban et al., 2020). Additionally, various yeasts (Leangnim, Aisara, Unban, Khanongnuch, & Kanpiengjai, 2021), lactic acid bacteria (LAB) (Cao et al., 2019) and *Bacillus* strains (Unban, Kodchasee, Shetty, & Khanongnuch, 2020) isolated from Miang and YDPT, have profound effect on chemical bio-conversion during the AF. Wen et al. (2023) revealed the formation of non-galloylated (non-ester) catechins, theaflavins and simple flavonols (non-glycosylated flavonols) along with the reduction of galloylated (ester) catechins and flavonol *O*-glycosides (glycosylated flavonols) during tea processing.

Nowadays, ultra-high performance liquid chromatography-triple quadrupole tandem mass spectrometry (UHPLC–QTrap–MS/MS)-based widely targeted metabolomics has revealed dynamic variation of metabolite profiles during tea processing (Xiao et al., 2022; Zhou et al., 2022). Besides high-performance liquid chromatography (HPLC) for quantitative determinations of several flavonoids, phenolic acids and caffeine, widely targeted metabolomics was applied to investigate dynamic change of non-volatile metabolites, and high throughput sequencing-based metagenomics was performed for bacterial and fungal community analysis during the AF of YDPT. Combined with multivariate statistical analyses, including principal component analysis (PCA), principal coordinate analysis (PCoA), hierarchical cluster analysis (HCA) and orthogonal least square discriminant analysis (OPLS-DA), this study aimed to elaborate characteristic metabolites variation and microbial community succession, and reveal biosynthesis mechanism of relevant flavonoids such as flavonols, flavones, flavanones and flavanonols during the AF.

2. Materials and methods

2.1. Chemical reagents

Five catechins, i.e., (+)-catechin (C, ≥ 98.0 %), (−)-epicatechin (EC, ≥ 98.0 %), (−)-epigallocatechin (EGC, ≥ 98.0 %), (−)-epicatechin gallate (ECG, ≥ 98.0 %), and (−)-epigallocatechin gallate (EGCG, ≥ 98.0 %), and two phenolic acids, namely gallic acid (GA, ≥ 98.0 %) and ellagic acid (EA, ≥ 98.0 %), and caffeine (≥ 98.0 %) were purchased from Yuanye Bio-Technology Co., Ltd. (Shanghai, China). Four flavonols including kaempferol (≥ 98 %), myricetin (≥ 99.0 %), quercetin (≥ 98.0 %) and rutin (quercetin-3-*O*-rutinoside, a flavonol *O*-glycoside, ≥ 98.0 %), and taxifolin (a flavanonol, ≥ 98.0 %) standards were purchased from Must Bio-Technology Co., Ltd. (Chengdu, Sichuan, China). Methanol, acetonitrile and *ortho*-phosphoric acid were purchased from CNM Technologies GmbH (Bielefeld, North Rhine-Westphalia, Germany). 2-Chloro-*L*-phenylalanine (≥ 98.0 %) and formic acid were purchased from Sigma-Aldrich Co., Ltd. (St. Louis, MO, USA).

2.2. Tea samples collected from the AF of YDPT

The AF was performed at Defeng Tea Industry Co., Ltd. of Dehong Dai and Jingpo Autonomous Prefecture in Yunnan Province, China for YDPT production. Fresh tea-leaves with one bud and two uppermost leaves of Yunnan Dayezhong variety (*Camellia sinensis* var. *assamica*) were harvested from ancient tea plantation with an age over 100 years. After spreading, fixation and rolling, these tea-leaves were used as raw material (RW) for AF according to a relevant proprietary technology (Patent number: ZL201510081460.6). The whole AF process lasted for nine months in a completely enclosed amphora at room temperature, during which tea samples were collected at two months (MFT2), four months (MFT4), six months (MFT6), eight months (MFT8), and nine months (MFT9), respectively. The collected tea samples were freeze-dried at −55 °C for 48 h using Genesis ES-55 Series (SP Scientific, Long Island, NY, USA) freeze dryer, and stored at −80 °C for metagenomics analysis. After sieving, tea powder with particles smaller than 425 μm was collected, and prepared for chemical analysis by HPLC and UHPLC-QTrap–MS/MS, respectively.

2.3. HPLC determination of ten flavonoids, two phenolic acids and caffeine

After extraction with 70 % (*v*/v) methanol solution for 24 h at 4 °C, five catechins, four flavonols and one flavanonol, and two phenolic acids and caffeine contents in tea samples were determined by an Agilent 1200 series HPLC system (Agilent Technologies, Santa Clara, CA, USA). The HPLC separation was achieved by using Poroshell 120 EC-C_{18} chromatogram column (100 × 4.6 mm, 2.7 μm; Agilent Technologies, Santa Clara, CA, USA) coupled with a Phenomenex C_{18} guard column (10 × 4.6 mm, 5 μm; Phenomenex, Torrance, CA, USA) (Hou et al., 2023). The gradient was programmed as follows: 0–16.0 min, 10 %–45 % B; 16.0–22.0 min, 45 %–65 % B; 25.0–25.9 min, 65 %–100 % B; 25.9–29.0 min, 100 % B; 29.0–30.0 min, 100 %–10 % B. The whole flow rate kept at 0.8 mL/min with a column temperature of 35 °C. The detection wavelengths were 280 nm (0–16 min) and 360 nm (16–30 min) (Ma et al., 2023). The analytical curves ($R^2 > 0.990$) were established to calculate their quantitative contents.

2.4. Tea extraction for widely targeted metabolomics

Tea powder (50 mg) was extracted with 700 μL of 75 % (*v*/v) methanol solution containing 2 μg/mL 2-chloro-*L*-phenylalanine as internal standard (Ma et al., 2021). Tea extraction procedure has been described in reports of Zhou et al. (2022) and Hou et al. (2023). Quality control (QC) samples were prepared by mixing an equal aliquot (20 μL) from each sample.

2.5. Widely targeted metabolomics by UHPLC–QTrap-MS/MS

The 2 μL of tea extraction was injected into an ExionLC AD System (Sciex Technologies, Framingham, MA, USA) with an ACQUITY UPLC HSS T3 column (100 × 2.1 mm, 1.8 μm; Waters Corporation, Milford, MA, USA) for UHPLC separation using 0.1 % formic acid solution (A) and acetonitrile (B) as the mobile phase (Hou et al., 2023). The gradient eluted program was as follows: 0–0.5 min, 2 % B; 0.5–10.0 min, 2 %–50 % B; 10.0–11.0 min, 50 %–95 % B; 11.0–13.0 min, 95 % B; 13.0–13.1 min, 95 %–2 % B; 13.1–15.0 min, 2 % B. The whole flow rate maintained at 0.4 mL/min with a column temperature of 40 °C. The QTrap 6500+ system Triple quadrupole mass spectrometer (Sciex Technologies, Framingham, MA, USA) equipped with IonDrive Turbo V electrospray ionization (ESI) source was applied for metabolite assay using multiple reaction monitoring (MRM) mode (Xiao et al., 2022). Metabolites were identified based on internal databases and public databases.

2.6. Metagenomics analysis for microbial community structure

2.6.1. DNA extraction and polymerase chain reaction (PCR)

Total genomic DNA was extracted by using Cetyltrimethyl ammonium bromide (CTAB)/Sodium dodecyl sulfate (SDS) method. The universal primers 341F (5′-CCTAYGGGRBGCASCAG-3′)/806R (5′-GGACTACNNGGGTATCTAAT-3′), and ITS5-1737F(5′-GGAAGTAAAAGTCGTAACAAGG-3′)/ITS2-2043R(5′-GCTGCGTTCTTCATCGATGC-3′) were used to amplify the V3-V4 hypervariable region of bacterial 16S rRNA genes and the ITS1-5F region of fungal 18S rRNA genes, respectively (Zhao et al., 2019). PCR was carried out with 15 μL of Phusion® High-Fidelity PCR Master Mix (New England Biolabs, Ipswich, MA, USA), 0.2 μM of forward and reverse primers, and 10 ng of template DNA. PCR amplification was carried out in an ABI 9700 Thermal Cycler (Applied Biosystems, Waltham, MA, USA) with the following thermal cycling parameters: initial denaturation at 98 °C for 1 min, followed by 30 cycles of denaturation at 98 °C for 10 s, annealing at 50 °C for 30 s, elongation at 72 °C for 30 s, and final extension at 72 °C for 5 min.

2.6.2. Illumina novaseq sequencing

The amplified PCR products were mixed with the same volume of

loading buffer, and were detected with 2 % (m/v) agarose gel. DNA fragments were purified with Qiagen Gel Extraction Kit (Qiagen, Hilden, North Rhine-Westphalia, Germany). The libraries were generated using the TruSeq® DNA PCR-Free Sample Preparation Kit (Illumina, San Diego, CA, USA) according to the manufacturer's instruction, and sequenced on an Illumina NovaSeq 6000 sequencing system (Illumina, San Diego, CA, USA).

2.6.3. Sequence analysis

FLASH software (Version 1.2.7), QIIME software (Version 1.9.1) and UCHIME Algorithm software were employed to obtain effective tags for sequence analysis. Sequences with ≥97 % similarity were assigned to the same operational taxonomic units (OTUs) using Uparse software (Version 7.0.1001). Species annotation and phylogenetic analysis were performed using Silva Database (http://www.arb-silva.de/) and MUSCLE software (Version 3.8.31), respectively. Using QIIME software (Version 1.7.0), α-diversity was assessed through six indices: observed-species, Chao1, Shannon, Simpson, ACE, and Good's coverage. Additionally, PCA, PCoA and non-metric multi-dimensional scaling (NMDS) were performed by using R software (Version 3.3.5, New zealand) for β-diversity analysis (Lin et al., 2022).

2.7. Statistical analysis

Three biological replications were carried out for data acquisition. One-way analysis of variance (ANOVA) using Tukey's honestly significant difference (HSD) test, the independent samples *t*-test and the correlation analysis were carried out by using SPSS 20.0 for Windows (Armonk, NY, USA) to acquire their significant difference levels and Spearman's correlation coefficients, respectively. PCA, HCA, heat map and volcano plots were performed by using Origin 9.0 software (Hampton, Massachusetts, USA). K-means clustering analysis was performed by using R software for Windows (Version 3.3.5). OPLS-DA was performed by using SIMCA-P 14.0 software (Umetrics, Umeå, Sweden). Based on characteristic metabolites selected by variable importance in the projection (VIP) > 1.0, $P < 0.05$, and fold change (FC) > 1.5 or < 0.67, metabolic pathway analysis was performed by using MetaboAnalyst 3.0 (http://www.metaboanalyst.ca/).

3. Results and discussion

3.1. Diversity analysis of microbial community structure

A total of 1,161,627 bacterial 16S rRNA and 1,142,064 fungal ITS

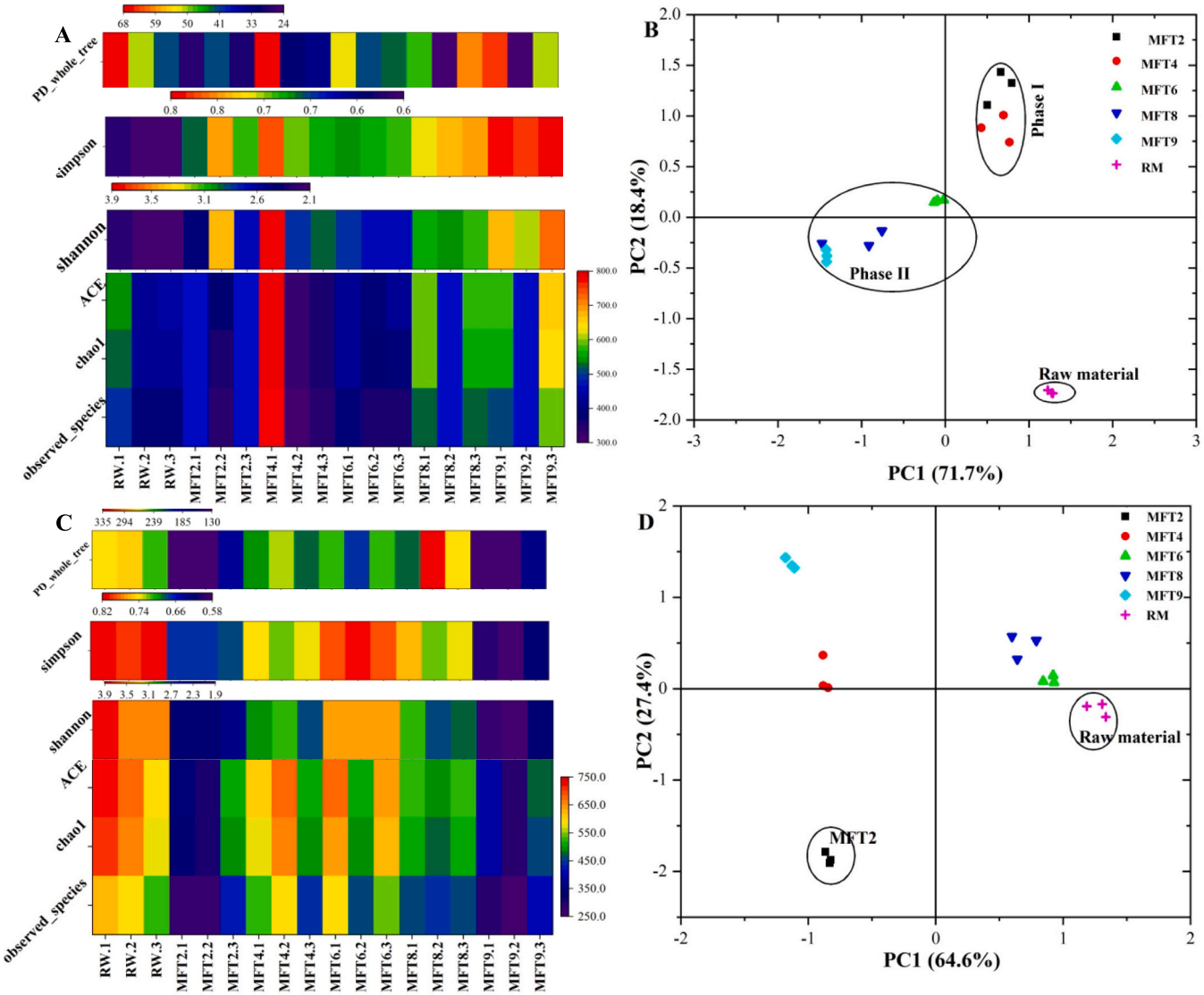

Fig. 1. α-diversity (A and C) and β-diversity (B and D) in bacterial (A and B) and fungal (C and D) community structures during the anaerobic fermentation, respectively.

sequences were obtained from six tea samples through Illumina NovaSeq sequencing, and clustered into 2314 bacterial and 2111 fungal OTUs (Fig. S1), respectively. All samples had good's coverage over 99.50 % (Table S1), indicating that their sufficient for microbiomics analysis. Because of a higher adaptation to anaerobic environment, bacterial community diversity evaluated by Shannon and Simpson, significantly ($P < 0.05$) increased, and bacterial community richness evaluated by Chao 1 and ACE, kept relatively stable during the whole AF (Fig. 1A and Table S1). Conversely, the rapid elimination of oxygen caused rapid and significant ($P < 0.05$) decrease of fungal community α-diversity during the first two months of AF, and then, the gradual adaptation to the anaerobic environment significantly ($P < 0.05$) improved fungal community diversity and richness after two months of AF (Fig. 1C and Table S1). Therefore, the AF exhibited a different α-diversity variation from aerobic fermentation, such as the pile-fermentation of RPT (Cheng et al., 2024; Zhao et al., 2019).

PCA, PCoA and NMDS have explored the β-diversity difference in microbial community structure during the pile-fermentation (Yan et al., 2021). In this study, NMDS confirmed the significant ($P < 0.05$) changes of bacterial (Stress = 0.083) and fungal (Stress = 0.126) OTUs during the AF (Fig. S2). Concretely, based on their bacterial community, the first two principal components (PC1 = 71.7 % and PC2 = 18.4 %) in PCA (Fig. 1B) divided these six tea samples into three groups, i.e., raw material (RW), Phase I (MFT2 and MFT4), and Phase II (MFT6, MFT8 and MFT9), which was consistent with PCoA result (Fig. S2B) that explained 91.32 % of total contribution (PCo1 = 82.13 % and PCo2 = 9.19 %). In contrast, PCA (Fig. 1D) and PCoA (Fig. S2D) elaborating about 92.00 % (PC1 = 64.6 % and PC2 = 27.4 %) and 87.32 % (PCo1 = 70.8 % and PCo2 = 16.52 %) of total variances in fungal community, respectively, both confirmed MFT2 as a separate group and other four AF samples (i.e. MFT4, MFT6, MFT8 and MFT9) as another group, which indicated a rapid variation of fungal community during the first two months.

3.2. Dynamic change of microbial community composition during the AF

3.2.1. Bacterial community succession

These bacterial OTUs were mainly classified into 47 phyla, and dominated by Cyanobacteria, Proteobacteria and Firmicutes in the relative abundance (RA). Cyanobacteria and Proteobacteria decreased rapidly from 58.34 % and 38.18 % to 25.00 % and 19.81 %, respectively, while Firmicutes steadily increased from less than 0.1 % to 19.09 % (MFT6), 28.65 % (MFT8) and 52.82 % (MFT9) in their RA (Fig. S3A). Among 396 annotated families, Lactobacillaceae continuously increased to 50.67 % (MFT9) from 0.06 % (RW) in RA, and became the predominant bacterial family in the AF (Fig. S3B), which have been reported to transform phenolics such as phenolic acids and flavonoids with multiple esterases and decarboxylases, as well as related reductases and glycosidases (Gaur & Gänzle, 2023). As facultative anaerobic bacteria, Enterobacteriaceae (1.7–30.0 %) showed rapid increase in Phase I, and obvious decrease in Phase II to 9.90 % (MFT9).

Among 628 annotated genera, 9 bacterial genera including *Lactiplantibacillus* (*Lactobacillus,* 0–32.7 %), *Klebsiella* (1.00–14.95 %), *Paucilactobacillus* (0–8.33 %), *Synechococcus*_CC9902 (0–3.15 %), *Secundilactobacillus* (0–4.94 %), *Pediococcus* (0–3.74 %),

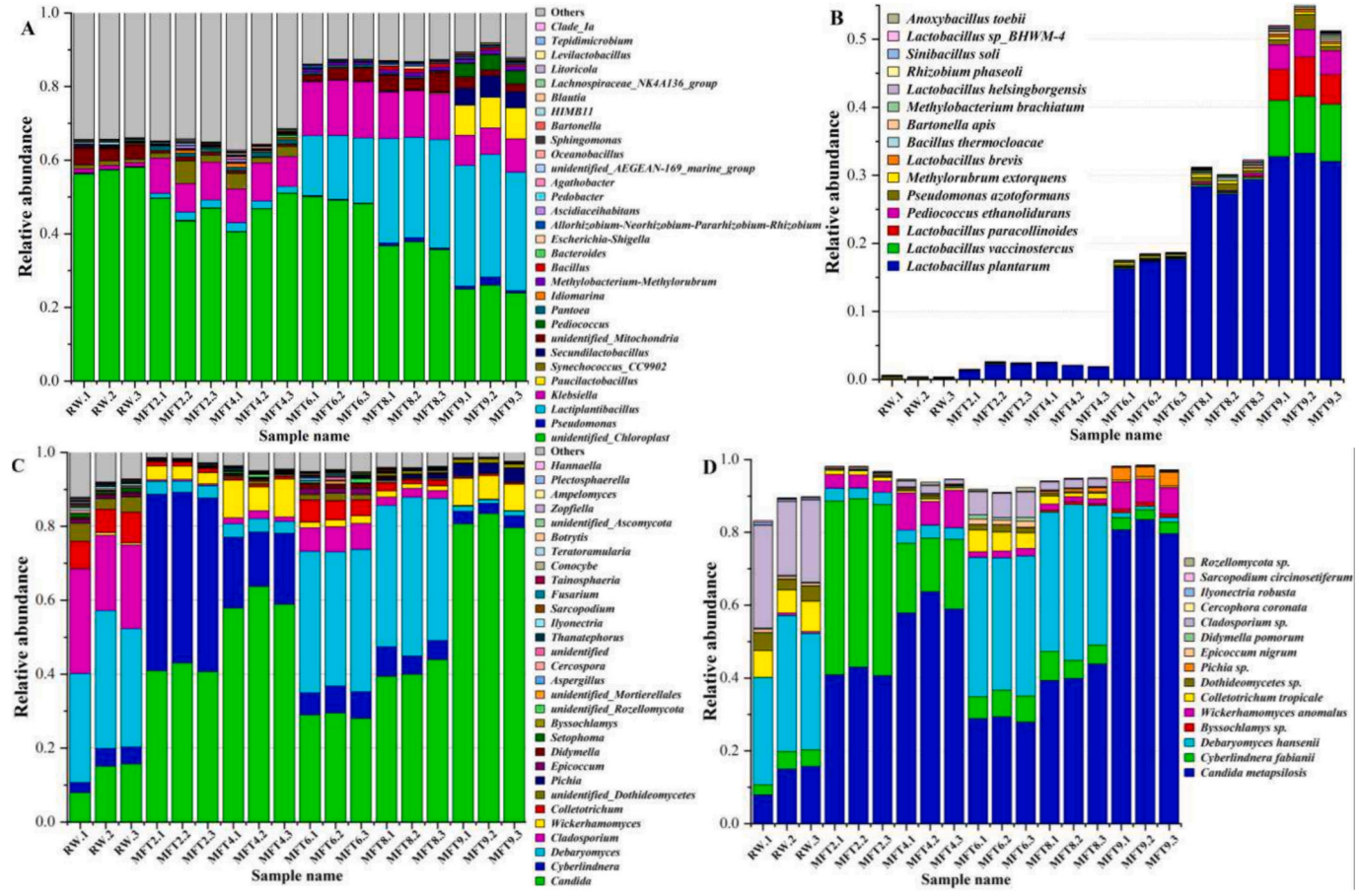

Fig. 2. Bacterial (A and B) and fungal (C and D) community succession during the anaerobic fermentation.
A: Top 30 genera in bacterial community and their dynamic changes during anaerobic fermentation.
B: Top 15 species in bacterial community and their dynamic changes during anaerobic fermentation.
C: Top 30 genera in fungal community and their dynamic changes during anaerobic fermentation.
D: Top 15 species in fungal community and their dynamic changes during anaerobic fermentation.

Methylobacterium-Methylorubrum (0.1–1.0 %) and *Pseudomonas* (0–1.0 %) and *Bacillus* (0–1.0 %) had a RA over 1 % (Fig. 2A). 12 Bacterial genera (i.e. *Lactiplantibacillus*, *Microbacterium*, *Bacillus*, *Allorhizobium-Neorhizobium-Pararhizobium-Rhizobium*, *Tepidimicrobium*, *Bartonella*, *Pediococcus*, *Methylobacterium-methylorubrum*, *Levilactobacillus*, *Secundilactobacillus* and *Paucilactobacillus*) showed increases along with decreases of *Pedobacter* and *Sphingomonas* during the AF (Fig. S3C). Additionally, 9 bacterial genera such as *Pantoea*, *Idiomarina*, *Ascidiaceihabitans*, *Halomonas* and *Litoricola* sharply increased in Phase I, and then showed continuous declines in Phase II. Particularly, *Lactiplantibacillus* increased rapidly from less than 0.1 % in RW to 32.72 % in MFT9, and became predominant bacterial genus, which was completely different from other dark teas dominated by *Ralstonia* (Zhang et al., 2020), *Pseudomonas* or *Bacillus* genera in the microbial fermentation (Le et al., 2023; Yan et al., 2021).

At the species level, *Lactiplantibacillus plantarum* (formerly *Lactobacillus plantarum*, 32.68 %), *Lactobacillus vaccinostercus* (8.33 %) and *Lactobacillus paracollinoides* (4.94 %) became dominant bacteria with dramatic increases during the AF (Fig. 2B). Additionally, multitudinous LAB such as *Lb. vaccinostercus*, *Lb. paracollinoides*, *Lactobacillus brevis*, *Lactobacillus helsingborgensis, Lactobacillus* sp_BHWM-4, *Lactobacillus apis, Lactobacillus reuteri, Lactobacillus murinus, Lactobacillus concavus, Lactobacillus salivarius, Pediococcus ethanolidurans, Pediococcus pentosaceus, Bifidobacterium_longum*, *Bifidobacterium_animalis*, and *Bifidobacterium_asteroides,* distinctly increased during the AF. Thereinto, as one of dominant LAB, *Lp. plantarum* has been identified in or isolated from anaerobic-fermented dark teas (Bo, Kim, & Han, 2020; Unban, Khatthongngam, et al., 2020; Unban, Kodchasee, et al., 2020), such as Laphet in Myanmar, Miang in Thailand, Ishizuchi-kurocha, Miyoshi and Awabancha in Japan. Particularly, twenty-four *Lp. plantarum*, one *Lactobacillus acidophilus* and one *Enterococcus casseliflavus* strains have been isolated from YDPT (Cao et al., 2019). Therefore, these LAB, particularly *Lp. plantarum,* might contribute to quality formation and chemical conversion in the AF, which deserves further investigation combined with metabolomics analysis.

3.2.2. Fungal community succession

These fungal OTUs were mainly classified into 14 phyla, 50 classes, 132 orders, 324 families, 639 genera and 888 species. As previously observed in the pile-fermentation (Zhao et al., 2019), Ascomycota (94.4–98.7 %) was superior in fungal community at the phylum level during the AF (Fig. S4A). Furthermore, incertae sedis Saccharomycetales (12.9–81.3 %) was confirmed as dominant fungal family (Fig. S4B), followed by Phaffomycetaceae (4.46–50.4 %), Debaryomycetaceae (1.23–39.9 %), Cladosporiaceae (0.04–23.97 %), Glomerellaceae (0.05–7.37 %) and Pichiaceae (0.08–3.37 %). Particularly, Phaffomycetaceae increased dramatically and became predominant fungal family in the MFT2 (50.4 %), but showed a rapid decrease to 10 % (MFT9). Additionally, Pichiaceae, Thermoascaceae, Didymellaceae, Leptosphaeriaceae, Sclerotiniaceae, Glomerellaceae, Tricholomataceae and Debaryomycetaceae showed obvious increases in the AF. Therefore, different from the predominance of filamentous fungi (mould) in aerobic-fermented dark teas (Le et al., 2023; Zhao et al., 2019), Saccharomycetales (yeast) dominated in the fungal community during the AF.

Among top 30 fungal genera, 12 decreased radically during the AF due to the anaerobic environment (Fig. S4C), such as *Teratoramularia*, *Cercospora*, *Sarcopodium*, *Setophoma*, *Plectosphaerella*, *Rachicladosporium*, *Ilyonectria*, *Paraphaeosphaeria* and *Cladosporium*, while *Pichia*, *Byssochlamys*, *Candida*, *Wickerhamomyces*, *Ampelomyces*, *Botrytis*, *Epicoccum* and *Didymella* showed remarkable increase after the six months. Thereinto, 11 fungal genera, including *Candida* (12.9–81.3 %), *Cyberlindnera* (3.1–46.9 %), *Debaryomyces* (1.2–39.9 %), *Cladosporium* (0.01–23.8 %), *Wickerhamomyces* (0.4–9.0 %), *Colletotrichum* (0.5–7.4 %), *unidentified_Dothideomycetes* (0.1–1.6 %), *Pichia* (0.1–3.4 %), *Epicoccum* (0.0–1.5 %), *Didymella* (0.1–1.1 %) and *Byssochlamys* (0.0–1.1 %), were over 1 % in the RA (Fig. 2C). Their rapid change was found in Phase I (MFT 2 and MFT4). For instance, *Cyberlindnera* increased drastically to 46.9 % in MFT2, and then decreased rapidly to 17.7 % in MFT4, along with the significant decrease of *Debaryomyces* from 32.9 % in RW to 3.4 % in MFT2. *Candida* and *Debaryomyces* increased to 41.1 % and 39.9 % in RA after the eight months, respectively, and became dominant fungal genera, which was completely different from the pile-fermentation of RPT and other dark teas (Cheng et al., 2024; Pan et al., 2023; Zhu et al., 2020). Conversely, *Aspergillus* was kept as low as below 1 % during the whole AF.

At the species level (Fig. 2D), *Candida metapsilosis* (12.9–81.3 %) was superior in RA, followed by *Cyberlindnera fabianii* (3.1–46.9 %) and *Debaryomyces hansenii* (1.2–39.8 %), which all were regarded as dominant yeasts during the AF. In addition, *Candida parapsilosis*, *Candida tropicalis*, *Candida quercitrusa*, *Candida anutae*, *Candida saitoana*, *Candida albicans*, *Cyberlindnera jadinii*, *Hyphopichia burtonii*, *Debaryomyces singareniensis* and *Pichia mandshurica* also were found in the AF. Generally, *Aspergillus niger* and *Aspergillus cristatus* (*Eurotium cristatum*) are critical fungi for quality formation of RPT and Fu-zhuan brick tea through relevant aerobic fermentation process, respectively (Ma et al., 2024). We speculated that these yeasts in the AF also promoted flavor formation and chemical conversion under the anaerobic environment, for chemical and flavor differences between RPT and YDPT.

3.3. Flavonoids transformation, and phenolic acids accumulation in AF detected by HPLC

The increasing trend of tea polyphenols content has been observed in whole AF process of pickled tea (Hou et al., 2023), which was completely different from the pile-fermentation with remarkable reduction of catechins to successively formulate thearubigins and theabrownins through oxidative polymerization (Ma et al., 2022). In this study, five catechins, four flavonols, taxifolin, two phenolic acids and caffeine contents were determined by HPLC to explore their dynamic changes during the AF. The PCA (Fig. 3A) could basically divide the whole AF process into phase I (i.e. before four months of AF) and phase II (i.e. after four months of AF) through the first two components (PC1 = 65.8 % and PC2 = 15.7 %). Heat map analysis (Fig. 3B) also could achieve the classification of AF phases, and cluster these chemical compounds into two groups. Specifically, caffeine, EC, EGC, kaempferol, quercetin, GA and EA showed continuous increases, while ECG, EGCG, rutin and myricetin showed obvious decreases during the AF. Additionally, the content of C and taxifolin also exhibited rapid change during the AF.

Generally, two non-galloylated catechins (i.e. EC and EGC), two non-glycosylated flavonols such as quercetin and kaempferol, and two phenolic acids highly significantly ($P < 0.01$) increased, along with the highly significant ($P < 0.01$) decreases of two galloylated catechins (i.e. ECG and EGCG) and rutin through one-way ANOVA (Fig. 3C), indicating that AF promoted flavonoids transformation such as catechins and flavonols, and the accumulation of phenolic acids. Caffeine content showed a highly significant ($P < 0.01$) increase at Phase I (MFT2 and MFT4), but then decreased ($P < 0.05$) at Phase II (MFT6, MFT8 and MFT9), which is consistent with the report by Wen et al. (2023). The C content showed a highly significant ($P < 0.01$) decrease after the two months, and then highly significantly ($P < 0.01$) increase after the six months.

During the AF, the galloylated catechins such as ECG and EGCG could be hydrolyzed into corresponding non-galloylated catechins (i.e. EC and EGC) and GA. The degradation of polymerized tannins, or the hydrolysis of galloyl glucose such as 1,3,6-trigalloyl glucose, also enhanced GA content, which could further be transformed into EA through oxypolymerization. The significant ($P < 0.05$) reduction of rutin might promote the formation of quercetin and kaempferol through hydrolyzation and further dehydroxylation (Huynh, Smagghe, Gonzales, van Camp, & Raes, 2016). Apart from hydrogenation, glycosylation, hydrolyzation and oxidation, the dehydroxylation/hydroxylation also

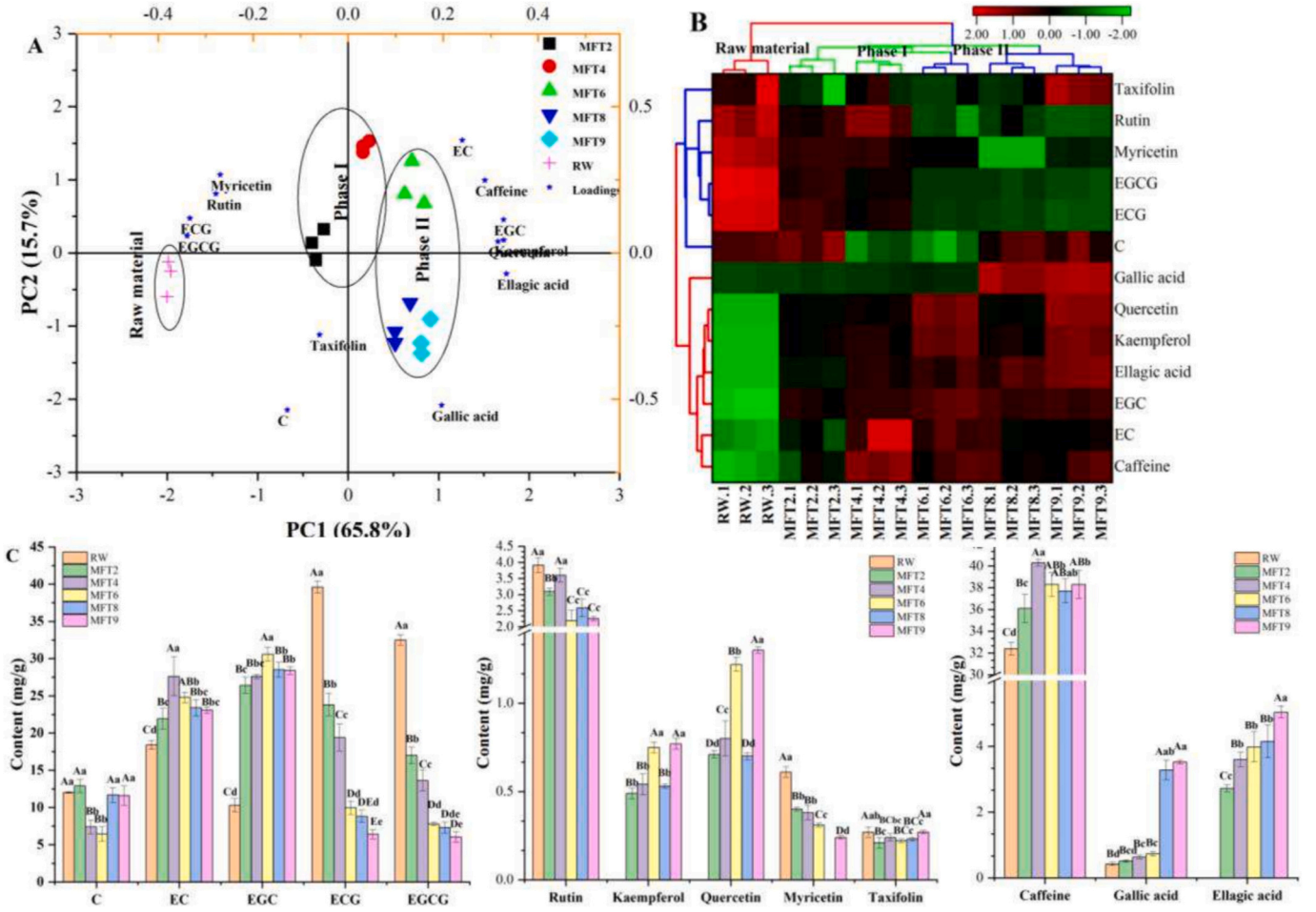

Fig. 3. Principal component analysis (PCA, A) divided the whole anaerobic fermentation into two phases, and heat map analysis (B) and one-way analysis of variance (ANOVA) displayed the dynamic changes of phenolics and purine alkaloids during the anaerobic fermentation.
Notes: C, (+)-catechin; EC, (−)-epicatechin, EGC, (−)-epigallocatechin; ECG, (−)-epicatechin gallate; EGCG, (−)-epigallocatechin gallate. ND indicates that the compounds such as ellagic acid, kaempferol and quercetin can not be detected in relevant tea samples by current HPLC method.
Different uppercase and lowercase letters in superscript (A, B to E, $P < 0.01$; a, b to e, $P < 0.05$) in the same row indicate levels of statically significant difference by one-way ANOVA using Tukey's honestly significant difference (HSD) test.

conduced to the mutual transformation among various flavonols. Particularly, myricetin can be transformed into quercetin through dehydroxylation, or laricitrin through *O*-methylatation, even 3,4,5-trihydroxyphenylacetic acid and phloroglucinol through the C-ring fission (Leonard, Zhang, Ying, Adhikari, & Fang, 2021). Therefore, the biosynthetic pathway of flavonols such as kaempferol and quercetin during the AF deserves further investigation.

3.4. Metabolite profiling of tea samples collected from AF

3.4.1. Multi/uni-variate statistical analyses

Among the 1253 detected metabolites, 976 metabolites with a relative content over 1 ppm calculated by their peak areas were selected for multi/uni-variate statistical analyses. These metabolites involved 376 phenolics (i.e. 167 flavonoids, 43 phenolic acids and their derivatives, 29 coumarins, 21 xanthones, 18 lignans, 11 quinones, 10 tannins, 27 phenols and 50 phenolic derivatives), 92 amino acids (such as 20 proteinogenic amino acids, 31 non-proteinogenic amino acids, 7 cyclic amino acids, 6 *N*-acetylated amino acids, 4 *N*-phenylacetylate amino acids, 4 *N*-formylated amino acids, 6 *N*-methylated amino acids and 4 oligopeptides), 89 organic acids (i.e. 21 aromatic organic acids, and 13 short-chain, 9 medium-chain and 46 long-chain fatty acids), 15 nucleotides, 23 nucleosides, 48 saccharides (i.e. 10 monosaccharides, 11 dis- and tri-accharides, 19 glycosides and 8 sugar derivatives), 136 alkaloids, 99 terpenoids (i.e. 17 monoterpenoids, 29 sesquiterpenoids, 30 diterpenoids and 23 tri/tetra-terpenoids), 47 sterides, 7 vitamins, 11 prenol lipids and 33 other metabolites (Fig. 4A). Particularly, as major phenolics, flavonoids including 17 flavanols, 44 flavones, 29 flavonols, 22 flavanones, 19 isoflavones, 13 chalcones, 10 flavanonols, 7 anthocyanidins and 6 other flavonoids, were dominant in content (65–74.0 %) and quantity (38.5 %), followed by amino acids and alkaloids.

The QC samples were located in the center of PCA (Fig. 4B), indicating method reliability for widely targeted metabolomics analysis. In PCA (Fig. 4B), the first two principal components explaining about 79.0 % of total variances (PC1 = 65.8 % and PC2 = 13.2 %), divided these six tea samples into three groups, i.e., raw material (RW), Phase I (MFT2 and MFT4) and Phase II (MFT6, MFT8 and MFT9), which was consistent with HPLC (Fig. 3A) and HCA results (Fig. 4C). One-way ANOVA (Table S2), heat map analysis (Fig. 4D) and K-mean clustering analysis (Fig. S5) were performed to elaborate dynamic change of non-volatile metabolites during the AF. The K-mean clustering analysis (Fig. S5) indicated profound changes of 384 metabolites, and divided these into nine clusters during the AF. Generally, 53 metabolites in cluster 1 and 62 metabolites in cluster 4 showed continuous increases, while 26 metabolites in cluster 3 and 37 metabolites in cluster 5 showed continuous decreases during the AF. Additionally, 70 metabolites in cluster 2 showed rapid increase in phase I and kept relatively stable in phase II.

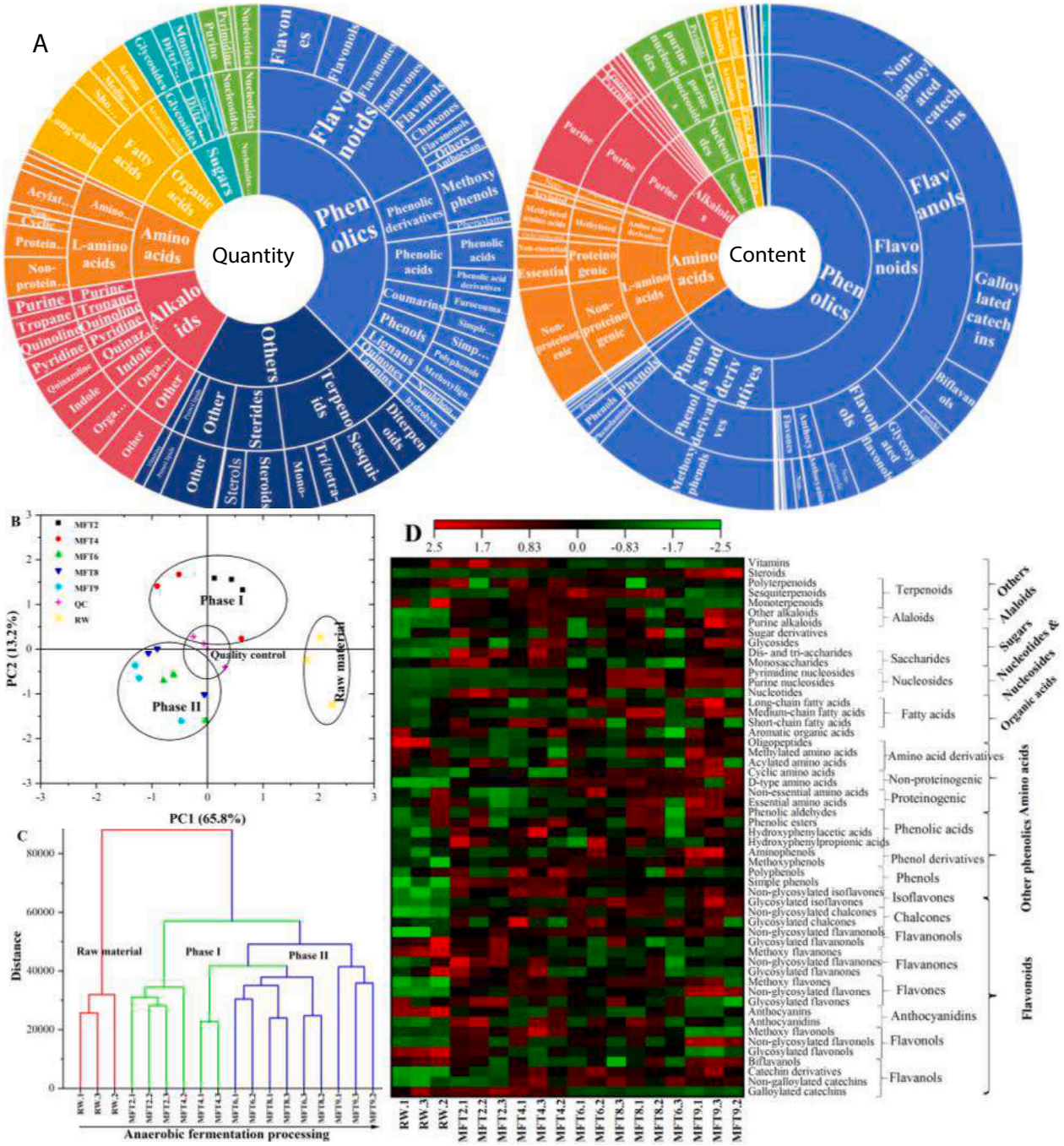

Fig. 4. Metabolites distributions (A) and their periodic changes during anaerobic fermentation through principal component analysis (PCA, B), hierarchical cluster analysis (HCA, C) and heat map analysis (D).

3.4.2. *Phenolics*

Completely different from its dramatic decrease during the pile-fermentation (Zhu et al., 2020), the total content of flavanols significantly ($P < 0.05$) increased in phase I due to its generation and liberation from food matrix, and then showed a significant decrease in phase II along with the significant ($P < 0.05$) decrease of galloylated catechins. Comparatively, the oxygen disappearance prevented the continuous oxidation and polymerization of theaflavin and non-galloylated catechins into thearubigins and theabrownins during the AF. Other than flavanols, the glycosylated forms dominated in flavonols, flavones, chalcones and anthocyanidins, including flavonol *O*-glycosides, anthocyanins, luteolin *O*-glycosides, and apigenin *C*-glycosides.

The hydrolyzation of flavonoid glycosides (glycosylated flavonoids) catalyzed by *β*-glucosidases and *α*-glucosidases (Ma, Ling, et al., 2021), enhanced simple (non-glycosylated) flavonols, flavones and chalcones, and anthocyanidins about 43.88, 25.93, 2.41 and 3.78 times after the AF, respectively. Conversely, the *C*-glycosylation in AF might enhance the contents of glycosylated forms of isoflavones and chalcones by 4.3 and 1.5 times, respectively. Additionally, the *O*-methoxylation multiplied methoxy flavones/flavonols contents in Phase I, and methoxy isoflavones content during the AF. In contrast, the hydrogenation of relevant flavones/flavonols such as apigenin, luteolin and quercetin, also significantly ($P < 0.05$) increased the levels of simple flavanones and flavanonols (Fig. 4D and Table S2).

As the second category of phenolics, phenols and their derivatives highly significantly ($P < 0.01$) increased along with the conversion of

insoluble tea polyphenols during the AF (Table S2). The *O*-methylation and amination of related phenols significantly ($P < 0.05$) improved methoxyphenols and aminophenols contents during the AF. Phenolic acids such as hydroxyphenylpropionic acids, hydroxyphenylacetic acids and hydroxybenzoic acids showed obvious increases during the AF (Fig. 4D and Table S2), which was mainly derived from the hydrolyzation of galloylated catechins (e.g. EGCG and ECG) and hydrolyzed tannins such as 1,3,6-tri-*O*-galloylglucose. Additionally, the other phenolics such as lignans, quinones, coumarins and xanthones, kept relatively stable with no significant ($P > 0.05$) change during the AF.

3.4.3. Amino acids

The hydrolyzation of water-soluble proteins into proteinogenic amino acids in phase II (Table S2), significantly ($P < 0.05$) enhanced total amino acids content during the AF, which was completely different from amino acids reduction and *N*-acetyl amino acids increase in the pile-fermentation (Chen et al., 2022). Notably, L-theanine hold steady in the AF for high umami taste of YDPT. However, during the pile-fermentation and the storage, L-theanine was converted into 1-ethyl-5-hydroxy-2-pyrrolidinone through intramolecular cyclization, and then formed into several 8-C *N*-ethyl-2-pyrrolidinone substituted flavan-3-ols (flavoalkaloids) through conjugation with the A-ring of non-galloylated

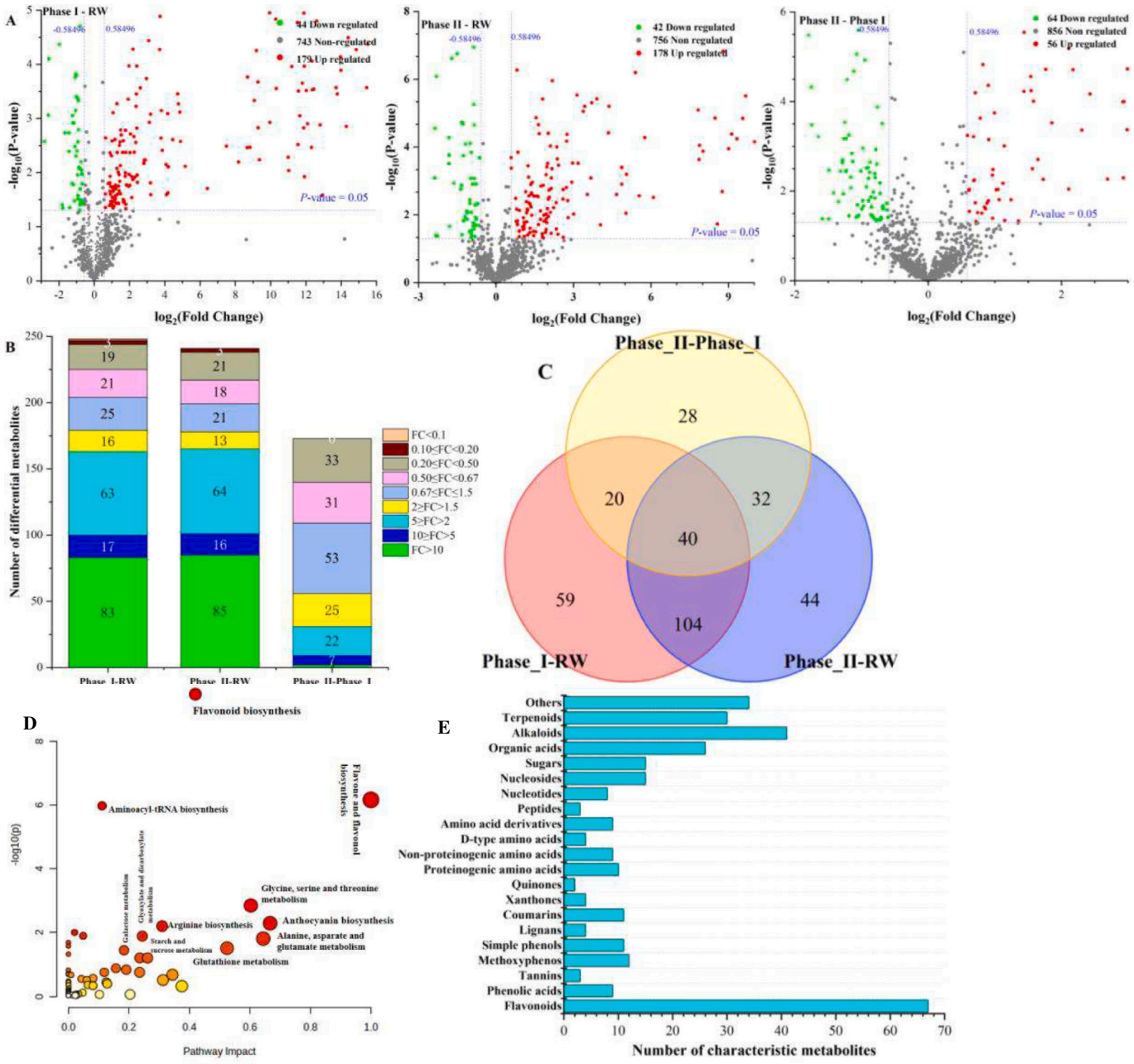

Fig. 5. Characteristic metabolites identified in anaerobic fermentation.
A: Volcano plots displayed up-regulated (VIP > 1.0, $P < 0.05$ and FC > 1.50) and down-regulated (VIP > 1.0, $P < 0.05$ and FC < 0.67) metabolites in three sets of comparisons, i.e., phase I-RW, phase II-RW and phase II-phase I, respectively, through orthogonal least square discriminant analysis (OPLS-DA).
B: Specific distributions of characteristic metabolites (VIP >1.0, $P < 0.05$, and FC > 1.50 or < 0.67) in three sets of comparisons.
C: Venn diagram exhibited the distribution of characteristic metabolites.
D: Pathway analysis of 327 characteristic metabolites selected in anaerobic fermentation.
E: Characteristic metabolites amount in each sub-class.

catechins (e.g. EC and EGC) (Wang et al., 2014). In addition, the AF also promoted massive accumulation of D-type amino acids by 4.52 times, such as D-α-aminobutyric acid and D-proline through the racemization of relevant amino acids.

3.4.4. Nucleosides and purine alkaloids

The AF promoted the continuous increase of nucleosides about 8-folds, and significant ($P < 0.05$) increase of nucleotides in phase I and their significant ($P < 0.05$) decrease in phase II, due to LAB and yeasts growth and metabolism. Chlorophyll decomposition and carbohydrate degradation induced the accumulation of total organic acids, particularly the significant ($P < 0.05$) increases of medium-chain and long-chain fatty acids. Soluble sugars such as monosaccharides, and di- and tri-accharides significantly ($P < 0.05$) or highly significantly ($P < 0.01$) increased in Phase I from the hydrolyzation of insoluble polysaccharides such as cellulose.

Purine alkaloids, occupying about 75.0 % of total alkaloids in content, demonstrated significant ($P < 0.05$) increases during the AF (Table S2), which was consistent with caffeine change. Particularly, the dramatic increase of 3-methylxanthine and 7-methylxanthine indicated purine alkaloids conversion during the AF. Generally, *Aspergillus sydowii*, *Aspergillus ustus* and *Aspergillus tamarii* isolated from the pile-fermentation of RPT promote the degradation or mutual transformation of caffeine, theobromine and theophylline through *N*-demethylation and oxidization (Zhou et al., 2020). We speculated that dominant microbes could be applied for methylxanthines production. Additionally, the terpenoids variation, particularly significant ($P < 0.05$) increase of sesquiterpenoids in phase I, might help to its fragrance formation.

3.5. Characteristic metabolites identified in the AF through OPLS-DA

The OPLS-DA acquired excellent discrimination in classification and identification of AF phases (Fig. S6 and Table S3). Among 976 metabolites, 179 up-regulated (VIP > 1.0, $P < 0.05$ and FC > 1.50) and 44 down-regulated (VIP > 1.0, $P < 0.05$ and FC < 0.67) metabolites were identified in the comparison of Phase I-RW, while 56 up-regulated and 64 down-regulated metabolites were identified in Phase II-Phase I, respectively (Fig. 5A). Particularly, 21 flavonoids, 14 phenols, 5 proteinogenic amino acids, 7 non-proteinogenic amino acids (e.g. 4 D-type amino acids), 7 sugars, 6 nucleosides & nucleotides and 14 alkaloids showed 10-folds increase during the AF (Fig. 5B). Furthermore, few novel characteristic metabolites (only 28) identified in Phase II-Phase I (Fig. 5C), indicated that the Phase I, i.e., the first four months was the major period for metabolites regulation during the AF. Overall, these 327 characteristic metabolites mainly involved in flavonoids metabolism, amino acid metabolism, and starch and sucrose metabolism through KEGG pathway analysis (Fig. 5D). Thereinto, 67 flavonoids (i.e. 18 flavonols, 14 flavones, 10 flavanones, 5 flavanols, 6 anthocyanins, 3 flavanonols, 5 chalcones, 4 isoflavones and 2 other flavonoids) were dominated in the characteristic metabolites, followed by alkaloids, amino acids, nucleotides, organic acids, sugars and phenolic acids (Fig. 5E), which confirmed the significant impact of AF on flavonoids conversion.

3.6. Flavonoids and phenolic acids variations during the AF

As most abundant secondary components and flavor substances, flavonoids and phenolic acids demonstrate profound changes during enzymatic fermentation in black tea processing through hydrolyzation, oxidation, ring fission and dehydroxylation (Liu, Vinchen, & de Bruijn, 2022). Furthermore, the microbial fermentation promoted catechin reduction for the generation of theabrownins and multitudinous catechin derivatives such as 8-carboxymethyl-(+)-catechin and puerins (Zhu et al., 2020), which was attributable to *Aspergillus* activity and their secreted extracellular enzymes such as polyphenol oxidase, peroxidase, pectinase, cellulase and laccase (Ma et al., 2024). The characteristic microbial community in the AF leaded to relative stability or increase of total phenolics content. Therefore, phenolics metabolism, particularly flavonoid conversion in the AF was explored based on characteristic phenolics as shown in Fig. S7 and Fig. S8. Among 17 flavanols, up-regulations of 3 flavanols, i.e., EGC, procyanidin A2 and (−)-epiafzelechin during the AF (Fig. S7), should be attributed to the secreted tannase that catalyzed the hydrolysis of galloylated catechins for non-galloylated catechins, GA and procyanidin A2 accumulations (Liu et al., 2020). Comparatively, the oxygen disappearance in the AF limited the continuous oxidation and polymerization of catechins to formulate theaflavins, thearubigins and theabrownins. Additionally, the dehydroxylation of EC might contribute to the up-regulation of (−)-epiafzelechin.

Except for flavanols, 18 among 29 detected flavonols showed profound variation during the AF. Thereinto, four kaempferol *O*-glycosides, four quercetin *O*-glycosides, myricitrin (myricetin 3-*O*-rhamnoside) and datiscetin obviously down-regulated for the mass accumulation of three simple flavanols (i.e. kaempferol, quercetin, myricetin), isorhamnetin (3-methylquercetin), two kaempferol *O*-glycosides (i.e. afzelin and kaempferitrin) and quercetin 3-*O*-glycosides during the AF (Fig. S7). Concretely, the simple flavonols were mainly derived from the hydrolyzation of relevant flavonol *O*-glycosides such as astragalin, isoquercitrin and myricitrin catalyzed by glycoside hydrolases such as β-glucosidase and α-glucosidase, which could improve health benefits of YDPT such as delaying decline in global cognition (Barreca et al., 2021; Holland et al., 2023). Generally, flavonoid 3′,5′-hydroxylase and flavonoid 3′-monooxygenase promoted hydroxylation/dehydroxylation among various flavonols. During the AF, hydroxylation/dehydroxylation could be found in between kaempferol and quercetin as well as their glycosides, and between quercetin and myricetin as well as their glycosides. Conversely, flavonoid 3′-monooxygenase catalyzed myricetin into quercetin, or quercetin into kaempferol through dehydroxylation, respectively. The *O*-methylation of quercetin by flavonoid *O*-transmethylase conduced the improvement of isorhamnetin over 20-folds. Furthermore, the *O*-glycosylation in the AF transformed kaempferol into afzelin and kaempferitrin. Similarly, the hydrolyzation of anthocyanins into anthocyanidins, and their mutual transformations also were found in the AF. The significant decrease of delphinidin-3-*O*-glucoside showed potential connections with the enhancements of two anthocyanidins (i.e. cyanidin and pelargonidin) and two anthocyanins (i.e. pelargonidin-3-*O*-glucoside and pelargonidin-3,5-*O*-diglucoside chloride) through hydrolyzation, dehydroxylation and glycosylation during the AF, which might impact infusion color of YDPT.

Among 44 detected flavones, three simple flavones (i.e. apigenin, scutellarein and tricetin), six methoxyflavones/methyoxyflavone *C*-glycosides (i.e. diosmetin, genkwanin, prunetin, tricin, isoscoparin and linarin) and homoorientin (luteolin-6-*C*-β-D-glucoside) showed up-regulations, along with down-regulations of four apigenin *C*-glycosides (i.e. meloside A, saponarin, vicenin 2 and vitexin 2″-glucoside) during the AF (Fig. S7), which confirmed that the AF promoted the hydrolyzation of apigenin *C*-glycosides, the *O*-methylation of flavones/flavone *C*-glycosides, and the *C*-glycosylation of luteolin. Particularly, the mass accumulation of tricetin about 30-folds, mainly came from the hydroxylation of luteolin or apigenin that was derived from the hydrolyzation of apigenin *C*-glycosides during the AF. Comparatively, AF also promoted the hydroxylation, *O*-methylation and *C*-glycosylation of relevant isoflavones for the up-regulations of 2′-hydroxygenistein, homoferreirin and puerarin. Particularly, the characteristic chalcones all showed significant up-regulation, due to the C-ring cleavage of flavanones, and subsequent reduction reaction and *O*-glycosylation. For instance, the C-ring cleavage of naringenin induced the accumulation of phloretin over 30-folds, which was further transformed into phlorizin through *O*-glycosylation, or chalconaringenin through reduction reaction, respectively. Correspondingly, non-glycosylated (simple) flavanones and flavanonols were dominated in total flavanones and flavanonols contents.

Therefore, the up-regulations of four simple flavanones (i.e. butin, eriodictyol, liquiritigenin and naringenin) and taxifolin, should be attributed to the reduction of simple flavones such as apigenin and luteolin, and flavonol (i.e. quercetin), and their mutual conversion through dehydroxylation/hydroxylation.

Nine phenolic acids and their derivatives, three tannins, thirteen coumarins, four lignans, four xanthones, three quinones, nine simple phenols and eleven methoxyphenols showed significant variations during the AF (Fig. S8). Apart from the hydrolyzations of galloylated catechins and tannins, the oxidation of hydroxybenzaldehydes such as protocatechualdehyde also generated hydroxybenzoic acids such as 3-hydroxybenzoic acid and GA during the AF. Similar to the pile-fermentation (Ge et al., 2019), the hydrolyzation of phenolic acid esters such as cynarin and chlorogenic acid promoted the enhancement of phenylpropionic acids such as *trans*-caffeic acid. The esterification in the AF significantly enhanced several phenolic acid esters such as methyl cinnamate, methyl gallate, methyl rosmarinate and methyl caffeate. Additionally, the decomposition and hydrolyzation of insoluble phenols, the *O*-methylation of coumarins and lignans, and the hydrolyzations or decompositions of coumarin glycosides and polylignans brought about phenolics increases during the AF. Overall, the accumulations of simple flavonols, flavones and flavanones, and their mutual bio-conversions through hydroxylation, hydrogenation, dehydroxylation, glycosylation and isomerization, found in the AF, was completely different from that in the pile-fermentation of RPT (Wang et al., 2022) and the AF of Miang (Chupeerach et al., 2021) and Hubei pickled tea (Zhang et al., 2020).

3.7. Flavonoids metabolism during the AF

Several *Aspergillus* such as *Aspergillus pallidofulvus* (Ma, Li, et al., 2021)*, Aspergillus sesamicola, Aspergillus tubingensis, Aspergillus fumigatus* and *A. sydowii* have been confirmed for the formation of theabrownins, puerins and simple flavonols such as kaempferol, quercetin and myricetin from oxidation, condensation and polymerization of catechins, and the hydrolyzation of flavonol glycosides (Wang et al., 2021). Additionally, the isolated yeasts such as *Sporidiobolus ruineniae, Cyberlindnera rhodanensis* and *Debaryomyces hansenii* also hydrolyze galloylated catechins into non-galloylated catechins through the production of cell-associated tannase (Leangnim et al., 2021). In this work, correlation analysis was executed to explore potential connections between dominant microbes and characteristic flavonoids based on their Spearman's correlation coefficients **(**Fig. 6A**)** for flavonoids metabolism during the AF. The synergistic effect between LAB and yeasts such as *Candida metapsilosis* and *Pichia* sp. could be found in the AF. For instance, the dominant LAB including *Lp. plantarum*, *Lb. vaccinostercus* and *Lb. paracollinoides* showed significantly positive ($r > 0.5$ and $P < 0.05$) correlations with relevant yeasts such as *Candida metapsilosis* and *Pichia* sp., which indicated that the massive growth of *Candida metapsilosis* within the first two months built up an appropriate environment for LAB breeding in the AF.

Their significant correlation coefficients ($|r| > 0.5$ and $P < 0.05$) between LAB and characteristic catechins (Fig. 6A), revealed that the LAB such as *Lp. plantarum* promoted the hydrolyzation of galloylated catechins into non-galloylated catechins, and (−)-epiafzelechin accumulation and theaflavin oxidization during the AF. Conversely, the impact of yeasts on catechins metabolism was relatively limited during the AF, due to that *Candida metapsilosis* only contributed to the enhancement of procyanidin A2. During the AF, both LAB and yeasts such as *Candida metapsilosis* and *Cyberlindnera fabianii* affected flavonol, flavone, flavanone, flavanonol, chalcone and anthocyanin metabolisms (Fig. S7 and Fig. S9), particularly the accumulation or generation of simple flavonols, isorhamnetin, 3 simple flavones (i.e. apigenin, scutellarein and tricetin), 3 methoxy-flavones (i.e. tricin, diosmetin and prunetin), simple flavanones (e.g. eriodictyol, naringenin, liquiritigenin and pinocembrin), homoorientin, phloretin, chalconaringenin, phlorizin and taxifolin through a sequence of biochemical reactions, such as the hydrolyzation, the *O*-methylation, the *C*-/*O*-glycosylation and the hydrogenation. Additionally, thirteen bacteria and four fungi might promote taxifolin formation with significantly positive correlations ($r > 0.5$ and $P < 0.05$), through the hydroxylation of eriodictyol or the hydrogenation of quercetin during the AF (Fig. S9). Comparatively, the yeasts such as *Candida metapsilosis*, *Cyberlindnera fabianii* and *Pichia* sp. conduced to the C-ring cleaving of naringenin into phloretin, while the LAB promoted the accumulations of chalconaringenin and asebogenin through the isomerization of naringenin and subsequent *O*-methylation.

Under synergistic effect of dominant LAB and yeasts, flavonoids pathway during the AF was speculated as shown in Fig. 6B. Generally, the continuous hydrolyzation of kaempferol-, quercetin- and apigenin-diglycosides including rutin, kaempferol-3-*O*-rutinoside, saponarin and vitexin 2″-glucoside, as well as the hydrolyzation of relevant flavonol monoglycosides including isoguercitrin, astragalin and myricitrin, formed kaempferol, quercetin, apigenin and myricetin, respectively. The hydroxylation/dehydroxylation promoted the mutual conversion among kaempferol, quercetin and myricetin as well as their glycosides. However, compared to the hydrolyzation of luteolin glycosides, the hydroxylation of apigenin induced the accumulation of luteolin, which could be further transformed into tricetin, diosmetin and homoorientin through hydroxylation, *O*-methylation or *C*-glycosylation, respectively. Additionally, apigenin, luteolin and quercetin could be reverted into naringenin, eriodictyol and taxifolin, respectively, by flavone/flavonol reductase. However, the *O*-glycosylation promoted kaempferol into afzelin and kaempferitrin in sequence, and phloretin into phlorizin, respectively. Except for the mutual conversion between naringenin and eriodictyol through hydroxylation/dehydroxylation, naringenin can be further transformed into phloretin and chalconaringenin through C-ring cleaving or isomerization. The *O*-methylation also occurred in quercetin, tricetin and phloretin to generate isohamnetin, tricin and asebogenin, respectively. Overall, the flavonoids bio-conversion mainly involved flavonoid 3′,5′-hydroxylase, flavonoid 3′-monooxygenase, glucoside hydrolases, flavonol *O*-glycosyltransferase, flavone *C*-glycosyltransferase, flavonoid *O*-transmethylase, flavone/flavonol reductase, flavanone/flavanol-cleaving reductase, flavanone 3-hydroxylase and chalcone isomerase released by relevant LAB and yeasts in the AF, which needs advanced researches.

4. Conclusions

In this work, LAB (e.g. *Lp. plantarum*, *Lb. vaccinostercus* and *Lb. paracollinoides*) and yeasts such as *Candida metapsilosis*, *Cyberlindnera fabianii* and *Debaryomyces hansenii*, were dominated in the AF of YDPT. The oxygen disappearance in the AF inhibited the growth of aerobic microorganism such as *Aspergillus* genus, but contributed to the growth and metabolism of relevant yeasts and LAB. Generally, the whole AF process could be divided into two phases, i.e. before and after four months through multivariate statistical analyses such as PCA and HCA. A total of 327 characteristic metabolites (VIP > 1.0, $P < 0.05$, and FC > 1.50 or < 0.67) were identified among 976 detected metabolites, which mainly involved flavonoids metabolism, amino acid metabolism, and starch and sucrose metabolism.

Besides amino acids, phenolic acids, phenols, sugars, nucleosides and purine alkaloids increases, the AF also promoted flavonoids bio-coversion. Particularly, the LAB and yeasts contributed to the accumulations of non-galloylated catechins, and simple flavones, flavonols and flavanones/flavanonols, and relevant methoxy flavones/flavonols, as well as the reductions of galloylated catechins, theaflavins, flavonol *O*-glycosides, apigenin glycosides and anthocyanins through hydrolyzation, hydroxylation, *O*-methylation, hydrogenation, oxidation and isomerization. Additionally, the *O*-glycosylation and *C*-glycosylation also were found in the AF for the generation of afzelin, kaempferitrin, phlorizin and homoorientin. These findings advanced the knowledge about AF mechanism of pickled tea and other dark tea, which would provide theoretical supports for AF technology innovation and

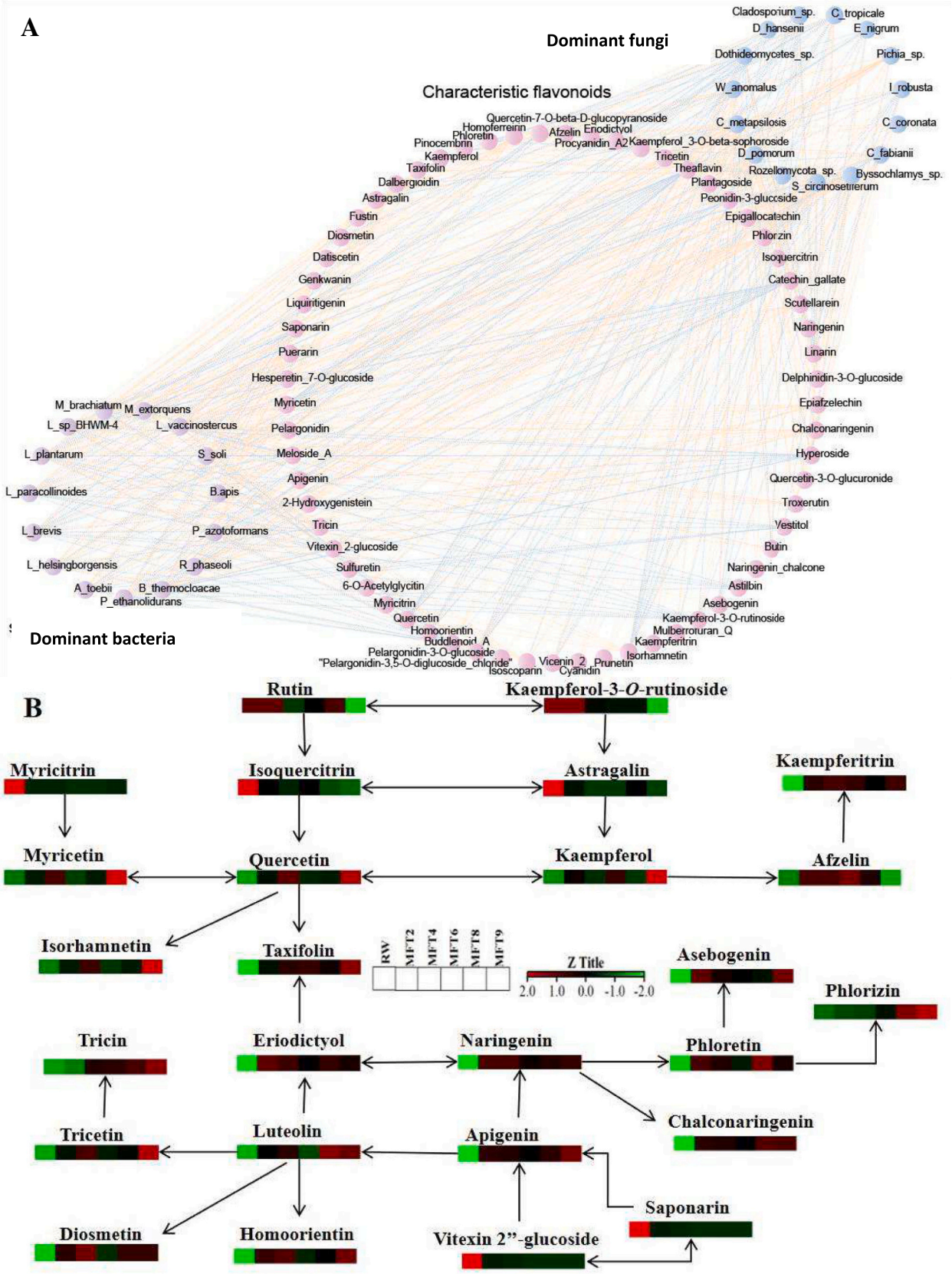

Fig. 6. Correlation analyses between characteristic flavonoids and dominant microbes (A), and relevant flavonoids pathways during the anaerobic fermentation (B). Note: The orange line indicated significant positive ($r > 0.5$ and $P < 0.05$) correlation, while the blue line indicated significant negative ($r < -0.5$ and $P < 0.05$). (For interpretation of the references to color in this figure legend, the reader is referred to the web version of this article.)

application of relevant effective microbe in dark tea production.

Ethics approval

The study did not involve any human or animal testing.

CRediT authorship contribution statement

Honglin Mao: Writing – review & editing, Writing – original draft, Validation, Investigation, Formal analysis, Conceptualization. **Yang Xu:** Writing – original draft, Visualization, Software, Data curation. **Fengmei Lu:** Resources, Investigation, Conceptualization. **Cunqiang Ma:** Writing – review & editing, Writing – original draft, Visualization, Software. **Shaoxian Zhu:** Methodology, Data curation. **Guoyou Li:** Investigation, Data curation. **Siqi Huang:** Resources, Formal analysis. **Yi Zhang:** Investigation. **Yan Hou:** Writing – review & editing, Project administration, Funding acquisition, Data curation.

Declaration of competing interest

The authors declare that they have no known competing financial interests or personal relationships that could have appeared to influence the work reported in this paper.

Data availability

Data will be made available on request.

Acknowledgements

This work was supported by the Cooperative Project of Yunnan Defeng Tea Industry Co. Ltd. (KX141721), the Agriculture Research System of China of Tea Industry Technology (CARS-19), and Yunnan Province Education Fund Project for Scientific Research (2021 J0110). We acknowledge Professor Wei Yuan and Professor Ming Zhao for their help in this study. In addition, we also thank Yunnan Defeng Tea Industry Co. Ltd., and Shanghai Biotree Biotech Co. Ltd. for their assistance in this study.

Appendix A. Supplementary data

Supplementary data to this article can be found online at https://doi.org/10.1016/j.fochx.2024.102021.

References

Barreca, D., Trombetta, D., Smeriglio, A., Mandalari, G., Romeo, O., Felice, M. R., … Nabavi, S. M. (2021). Food flavonols: Nutraceuticals with complex health benefits and functionalities. *Trends in Food Science & Technology, 117*, 194–204.

Bo, B., Kim, S. A., & Han, N. S. (2020). Bacterial and fungal diversity in Laphet, traditional fermented tea leaves in Myanmar, analyzed by culturing, DNA amplicon-based sequencing, and PCR-DGGE methods. *International Journal of Food Microbiology, 320*, Article 108508. https://doi.org/10.1016/j.ijfoodmicro.2020.108508

Cao, Z.-H., Pan, H.-B., Li, S.-J., Shi, C.-Y., Wang, S.-F., Wang, F.-Y., … Z.-Y.. (2019). *In vitro* evaluation of probiotic potential of lactic acid bacteria isolated from Yunnan De'ang pickled tea. *Probiotics and Antimicrobial Proteins, 11*, 103–112. https://doi.org/10.1007/s12602-018-9395-x

Chen, S., Fu, Y., Bian, X., Zhao, M., Zou, Y., Ge, Y., , … Wu, & J.-L.. (2022). Investigation and dynamic profiling of oligopeptides, free amino acids and derivatives during Pu-erh tea fermentation by ultra-high performance liquid chromatography tandem mass spectrometry. *Food Chemistry, 371*, Article 131176. https://doi.org/10.1016/j.foodchem.2021.131176

Cheng, L.-Z., Yang, Q.-Q., Peng, L.-L., Xu, L.-R., Chen, J.-H., Zhu, Y.-Z., & Wei, X.-L. (2024). Exploring core functional fungi driving the metabolic conversion in the industrial pile fermentation of Qingzhuan tea. *Food Research International, 178*, Article 113979. https://doi.org/10.1016/j.foodres.2024.113979

Chupeerach, C., Aursalung, A., Watcharachaisoponsiri, T., Whanmek, K., Thiyajai, P., Yosphan, K., … Suttisansanee, U. (2021). The effect of steaming and fermentation on nutritive values, antioxidant activities, and inhibitory properties of tea leaves. *Foods, 10*(1), 117. https://doi.org/10.1111/1541-4337.13051

Gaur, G., & Gänzle, M. G. (2023). Conversion of (poly)phenolic compounds in food fermentations by lactic acid bacteria: Novel insights into metabolic pathways and functional metabolites. *Current Research in Food Science, 6*, Article 100448. https://doi.org/10.1016/j.crfs.2023.100448

Ge, Y., Bian, X., Sun, B., Zhao, M., Ma, Y., Tang, Y., , … Wu, & J.-L.. (2019). Dynamic profiling of phenolic acids during Pu-erh tea fermentation using derivatization liquid chromatography–mass spectrometry approach. *Journal of Agricultural and Food Chemistry, 67*(16), 4568–4577. https://doi.org/10.1021/acs.jafc.9b00789

Holland, T. M., Agarwal, P., Wang, Y. M., Dhana, K., Leutgans, S. E., Shea, K., … Barnes, L. L. (2023). Association of dietary intake of flavonols with changes in global cognition and several cognitive abilities. *Neurology, 100*(7). e694-e672.

Hou, Y., Mao, H.-L., Lu, F.-M., Ma, C.-Q., Zhu, S.-X., Li, G.-Y., , … Xiao, & R.. (2023). Widely targeted metabolomics and HPLC analysis elaborated the quality formation of yunnan pickled tea during the whole process at an industrial scale. *Food Chemistry, 422*, Article 135716. https://doi.org/10.1016/j.foodchem.2023.135716

Huynh, N. T., Smagghe, G., Gonzales, G. B., van Camp, J., & Raes, K. (2016). Extraction and bioconversion of kaempferol metabolites from cauliflower outer leaves through fungal fermentation. *Biochemical Engineering Journal, 116*, 27–33. https://doi.org/10.1016/j.bej.2015.12.005

Le, M.-M., Zhong, L.-W., Ren, Z.-W., An, M.-Q., Long, Y.-H., & Ling, T.-J. (2023). Dynamic changes in the microbial community and metabolite profile during the pile fermentation process of fuzhuan brick tea. *Journal of Agricultural and Food Chemistry, 71*(48), 19142–19153. https://doi.org/10.1021/acs.jafc.3c04459

Leangnim, N., Aisara, J., Unban, K., Khanongnuch, C., & Kanpiengjai, A. (2021). Acid stable yeast cell-associated tannase with high capability in gallated catechin biotransformation. *Microorganisms, 9*, 1418. https://doi.org/10.3390/microorganisms9071418

Leonard, W., Zhang, P.-Z., Ying, D.-Y., Adhikari, B., & Fang, Z.-X. (2021). Fermentation transforms the phenolic profiles and bioactivities of plant-based foods. *Biotechnology Advances, 49*, Article 107763.

Lin, F.-J., Wei, X.-L., Liu, H.-Y., Li, H., Xia, Y., Wu, D.-T., , … Gan, & R.-Y.. (2021). State-of-the-art review of dark tea: From chemistry to health benefits. *Trends in Food Science & Technology, 109*, 126–138. https://doi.org/10.1016/j.tifs.2021.01.030

Lin, Y., Yu, W.-T., Cai, C.-P., Wang, P.-J., Gao, S.-L., Zhang, J.-M., , … Ye, & N.-X.. (2022). Rapid varietal authentication of oolong tea products by microfluidic-based SNP genotyping. *Food Research International, 162*, Article 111970. https://doi.org/10.1016/j.foodres.2022.111970

Liu, M.-L., Xie, H.-F., Ma, Y., Li, H.-Y., Li, C.-P., Chen, L.-J., … Zhao, M. (2020). High performance liquid chromatography and metabolomics analysis of tannase metabolism of gallic acid and gallates in tea leaves. *Journal of Agricultural and Food Chemistry, 68*, 4946–4954.

Liu, Z.-B., Vinchen, J. P., & de Bruijn, W. J. (2022). Tea phenolics as prebiotics. *Trends in Food Science & Technology, 127*, 156–168. https://doi.org/10.1016/j.tifs.2022.06.007

Ma, C.-Q., Li, X.-H., Zheng, C.-Q., Zhou, B.-X., Xu, C.-C., & Xia, T. (2021). Comparison of characteristic components in tea-leaves fermented by *aspergillus pallidofulvus* PT-3, *aspergillus sesamicola* PT-4 and *Penicillium manginii* PT-5 using LC-MS metabolomics and HPLC analysis. *Food Chemistry, 350*, Article 129228. https://doi.org/10.1016/j.foodchem.2021.129228

Ma, C.-Q., Ma, B.-S., Zhou, B.-X., Xu, L.-J., Hu, Z.-H., Li, X.-H., & Chen, X. (2024). Pile-fermentation mechanism of ripened Pu-erh tea: Omics approach, chemical variation and microbial effect. *Trends in Food Science & Technology, 146*, Article 104379. https://doi.org/10.1016/j.tifs.2024.104379

Ma, C.-Q., Zhou, B.-X., Wang, J.-C., Ma, B.-S., Lv, X., Chen, X., & Li, X.-H. (2023). Investigation and dynamic changes of phenolic compounds during a new-type fermentation for ripened Pu-erh tea processing. *LWT- Food Science and Technology, 180*, Article 114683. https://doi.org/10.1016/j.lwt.2023.114683

Ma, Y., Jiang, B., Liu, K., Li, R., Chen, L., Liu, Z., … M.. (2022). Multi-omics analysis of the metabolism of phenolic compounds in tea leaves by *aspergillus luchuensis* during fermentation of pu-erh tea. *Food Research International, 162*, Article 111981.

Ma, Y., Ling, T., Su, X., Jiang, B., Nian, B., Chen, L.-J., … Zhao, M. (2021). Integrated proteomics and metabolomics analysis of tea leaves fermented by *aspergillus Niger*, *aspergillus tamarii* and *aspergillus fumigatus*. *Food Chemistry, 334*, Article 127560. https://doi.org/10.1016/j.foodchem.2020.127560

Pan, J. C., Wang, J., Teng, J.-W., Huang, L., Wei, B.-Y., Xia, N., & Zhu, P.-C. (2023). Deciphering the underlying core microorganisms and the marker compounds of Liupao tea during the pile-fermentation process. *Journal of the Science of Food and Agriculture, 104*(5), 2862–2875. https://doi.org/10.1002/jsfa.13177

Unban, K., Khatthongngam, N., Pattananandechamm, T., Saenjum, C., Shetty, K., & Khanongnuch, C. (2020). Microbial community dynamics during the non-filamentous fungi growth-based fermentation process of *Miang*, a traditional fermented tea of north Thailand and their product characterizations. *Frontiers in Microbiology, 11*, 1515. https://doi.org/10.3389/fmicb.2020.01515

Unban, K., Kodchasee, P., Shetty, K., & Khanongnuch, C. (2020). Tannin-tolerant and extracellular tannase producing *Bacillus* isolated from traditional fermented tea leaves and their probiotic functional properties. *Foods, 9*, 490. https://doi.org/10.3390/foods9040490

Wang, W., Zhang, L., Wang, S., Shi, S., Jiang, Y., Li, N., & Tu, P. (2014). 8-C *N*-ethyl-2-pyrrolidinone substituted flavan-3-ols as the marker compounds of Chinese dark teas formed in the post-fermentation process provide significant antioxidative activity. *Food Chemistry, 152*, 539–545. https://doi.org/10.1016/j.foodchem.2013.10.117

Wang, X., Li, N., Chen, S.-S., Ge, Y.-H., Xiao, Y., Zhao, M., et al. (2022). MS-FINDER assisted in understanding the profile of flavonoids in temporal dimension during the fermentation of Pu-erh tea. *Journal of Agricultural and Food Chemistry, 70*, 7085–7094.

Wang, Z., Zheng, C., Ma, C., Ma, B., Wang, J., Zhou, B., & Xia, T. (2021). Comparative analysis of chemical constituents and antioxidant activity in tea-leaves microbial fermentation of seven tea-derived fungi from ripened Pu-erh tea. *LWT- Food Science and Technology, 142*, Article 111006. https://doi.org/10.1016/j.lwt.2021.111006

Wen, M.-C., Zhou, F., Zhu, M.-T., Han, Z.-S., Lai, G.-P., Jiang, Z.-D., , … Zhang, & L.. (2023). Monitoring of pickled tea during processing: From LC-MS based metabolomics analysis to inhibitory activities on α-amylase and α-glycosidase. *Journal of Food Composition and Analysis, 117*, Article 105108. https://doi.org/10.1016/j.jfca.2022.105108

Xiao, Y., He, C., Chen, Y., Ho, C.-T., Wu, X., Huang, Y., , … Liu, & Z.. (2022). UPLC–QQQ–MS/MS-based widely targeted metabolomic analysis reveals the effect of solid-state fermentation with *Eurotium cristatum* on the dynamic changes in the metabolite profile of dark tea. *Food Chemistry, 378*, Article 131999. https://doi.org/10.1016/j.foodchem.2021.131999

Xu, J., Wei, Y., Li, F.-L., & Wei, X.-L. (2022). Regulation of fungal community and the quality formation and safety control of Pu-erh tea. *Comprehensive Reviews in Food Science and Food Safety, 21*(6), 4546–4572.

Yan, K., Yan, L.-F., Meng, L.-N., Cai, H.-B., Duan, A.-L., Wang, L., … Abbas, M. (2021). Comprehensive analysis of bacterial community structure and diversity in Sichuan dark tea (*Camellia sinensis*). *Frontiers in Microbiology, 12*, Article 735618. https://doi.org/10.3389/fmicb.2021.735618

Zhang, H., Liu, Y.-Z., Xu, W.-C., Chen, W.-J., Wu, S., & Huang, Y.-L. (2020). Metabolite and microbiome profilings of pickled tea elucidate the role of anaerobic fermentation in promoting high levels of gallic acid accumulation. *Journal of Agricultural and Food Chemistry, 68*, 13751–13759. https://doi.org/10.1021/acs.jafc.0c06187

Zhang, M.-M., Otake, K., Miyauchi, Y., Yagi, M., Yonei, Y., Miyakawa, T., & Tanokura, M. (2019). Comprehensive NMR analysis of two kinds of post-fermented tea and their anti-glycation activities *in vitro*. *Food Chemistry, 277*, 735–743. https://doi.org/10.1016/j.foodchem.2018.11.028

Zhao, M., Su, X.-Q., Nian, B., Chen, L.-J., Zhang, D.-L., Duan, S.-M., … Ma, Y. (2019). Integrated meta-omics approaches to understand the microbiome of spontaneous fermentation of traditional Chinese pu-erh tea. *mSystems, 4*(6), Article e00680. –19 https://doi.org/10.1128/mSystems.00680-19.

Zhou, B., Ma, C., Xia, T., Li, X., Zheng, C., Wu, T., & Liu, X. (2020). Isolation, characterization and application of theophylline-degrading *aspergillus* fungi. *Microbial Cell Factories, 19*, 72. https://doi.org/10.1186/s12934-020-01333-0

Zhou, J., Fang, T., Li, W., Jiang, Z., Zhou, T., Zhang, L., & Yu, Y. (2022). Widely targeted metabolomics using UPLC-QTRAP-MS/MS reveals chemical changes during the processing of black tea from the cultivar *Camellia sinensis* (L.) O. Kuntze cv. Huangjinya. *Food Research International, 162*, Article 112169. https://doi.org/10.1016/j.foodres.2022.112169

Zhu, M., Li, N., Zhou, F., Ouyang, J., Lu, D., Xu, W., , … Wu, & J.. (2020). Microbial bioconversion of the chemical components in dark tea. *Food Chemistry, 312*, Article 126043. https://doi.org/10.1016/j.foodchem.2019.126043